

**Are your MRI contrast agents cost-effective?**

Learn more about generic Gadolinium-Based Contrast Agents.



**AJNR**

This information is current as  
of April 18, 2024.

## **Diffusion Tensor Imaging Mapping of Brain White Matter Pathology in Mitochondrial Optic Neuropathies**

D.N. Manners, G. Rizzo, C. La Morgia, C. Tonon, C. Testa,  
P. Barboni, E. Malucelli, M.L. Valentino, L. Caporali, D.  
Strobbe, V. Carelli and R. Lodi

*AJNR Am J Neuroradiol* 2015, 36 (7) 1259-1265

doi: <https://doi.org/10.3174/ajnr.A4272>

<http://www.ajnr.org/content/36/7/1259>

# Diffusion Tensor Imaging Mapping of Brain White Matter Pathology in Mitochondrial Optic Neuropathies

D.N. Manners, G. Rizzo, C. La Morgia, C. Tonon, C. Testa, P. Barboni, E. Malucelli, M.L. Valentino, L. Caporali, D. Strobbe, V. Carelli, and R. Lodi



## ABSTRACT

**BACKGROUND AND PURPOSE:** Brain white matter is frequently affected in mitochondrial diseases; *optic atrophy gene 1*-autosomal dominant optic atrophy and Leber hereditary optic neuropathy are the most frequent mitochondrial monosymptomatic optic neuropathies. In this observational study, brain white matter microstructure was characterized by DTI in patients with *optic atrophy gene 1*-autosomal dominant optic atrophy and Leber hereditary optic neuropathy, in relation to clinical and genetic features.

**MATERIALS AND METHODS:** Nineteen patients with *optic atrophy gene 1*-autosomal dominant optic atrophy and 17 with Leber hereditary optic neuropathy older than 18 years of age, all genetically diagnosed, and 19 healthy volunteers underwent DTI by using a 1.5T MR imaging scanner and neurologic and ophthalmologic assessments. Brain white matter DTI metrics were calculated for all participants, and, in patients, their correlations with genetics and clinical findings were calculated.

**RESULTS:** Compared with controls, patients with *optic atrophy gene 1*-autosomal dominant optic atrophy had an increased mean diffusivity in 29.2% of voxels analyzed within major white matter tracts distributed throughout the brain, while fractional anisotropy was reduced in 30.3% of voxels. For patients with Leber hereditary optic neuropathy, the proportion of altered voxels was only 0.5% and 5.5%, respectively, of which half was found within the optic radiation and 3.5%, in the smaller acoustic radiation. In almost all regions, fractional anisotropy diminished with age in patients with *optic atrophy gene 1*-autosomal dominant optic atrophy and correlated with average retinal nerve fiber layer thickness in several areas. Mean diffusivity increased in those with a missense mutation. Patients with Leber hereditary optic neuropathy taking idebenone had slightly milder changes.

**CONCLUSIONS:** Patients with Leber hereditary optic neuropathy had preferential involvement of the optic and acoustic radiations, consistent with trans-synaptic degeneration, whereas patients with *optic atrophy gene 1*-autosomal dominant optic atrophy presented with widespread involvement suggestive of a multisystemic, possibly a congenital/developmental, disorder. White matter changes in Leber hereditary optic neuropathy and optic atrophy gene 1-autosomal dominant optic atrophy may be exploitable as biomarkers.

**ABBREVIATIONS:** DOA = autosomal dominant optic atrophy; FA = fractional anisotropy; LHON = Leber hereditary optic neuropathy; MD = mean diffusivity; OPA1 = *optic atrophy gene 1*; OR = optic radiation; RNFL = retinal nerve fiber layer; TBSS = tract-based spatial statistics

Mutations in *optic atrophy gene 1* are the main cause of autosomal dominant optic atrophy (DOA) (Online Mendelian Inheritance in Man 605290).<sup>1,2</sup> DOA is characterized clinically by insidiously progressive visual loss in childhood, centrocecal sco-

toma, dyschromatopsia, and temporal or diffuse pallor of the optic discs, due to selective loss of retinal ganglion cells leading to atrophy of the optic nerve.<sup>1,2</sup> Similarly, Leber hereditary optic neuropathy (LHON) (Online Mendelian Inheritance in Man 535000) is characterized by subacute loss of central vision, dyschromatopsia, and optic atrophy due to maternally inherited

Received October 2, 2014; accepted after revision December 5.

From the Functional MR Unit (D.N.M., G.R., C.Tonon, C.Testa, R.L.) and Neurology Unit (G.R., C.L.M., M.L.V., L.C., D.S., V.C.), Department of Biomedical and NeuroMotor Sciences, and Department of Pharmacy and Biotechnology (E.M.), University of Bologna, Bologna, Italy; "Istituto di Ricovero e Cura a Carattere Scientifico Istituto delle Scienze Neurologiche di Bologna" (C.L.M., M.L.V., L.C., D.S., V.C.), Bologna, Italy; and Studio Oculistico d'Azeglio (P.B.), Bologna, Italy.

D.N. Manners and G. Rizzo contributed equally to this work.

The work was financially supported, in part, by Telethon-Italy grants GGP06233 and GPP10005 and the E-RARE project ERMION: 01GM1006. The funding organizations played no part in the design or conduct of the study; collection, management, analysis, or interpretation of the data; or in the preparation, review, or approval of the article.

Please address correspondence to Raffaele Lodi, MD, Functional MR Unit, Department of Biomedical and NeuroMotor Sciences, Via Massarenti 9, 40138 Bologna, Italy; e-mail: raffaele.lodi@unibo.it; Valerio Carelli, MD, PhD, IRCCS Istituto delle Scienze Neurologiche di Bologna, Ospedale Bellaria, Via Altura 3, 40139 Bologna, Italy; e-mail: valerio.carelli@unibo.it

Indicates open access to non-subscribers at [www.ajnr.org](http://www.ajnr.org)

Indicates article with supplemental on-line tables.

Indicates article with supplemental on-line photo.

<http://dx.doi.org/10.3174/ajnr.A4272>

point mutations in mitochondrial DNA that affect respiratory complex I.<sup>1,2</sup>

DOA and LHON represent the so-called nonsyndromic mitochondrial optic neuropathies, characterized by optic nerve atrophy as the only or at least prevalent pathologic feature with an early and preferential involvement of the small fibers in the papillomacular bundle.<sup>3,4</sup> Recent MR imaging studies by using voxel-based morphometry,<sup>5</sup> DWI,<sup>6</sup> and DTI<sup>7</sup> have also indicated abnormalities of the optic radiation in patients with LHON, confirmed by postmortem investigation,<sup>6</sup> suggesting a trans-synaptic degeneration. A similar secondary involvement of the retrogeniculate visual pathway could also be hypothesized in patients with DOA. Furthermore, given that the *optic atrophy gene 1* (*OPA1*) is highly expressed in the retina but also in the brain<sup>1,2,8</sup> and that a subgroup of patients with specific *OPA1* mutations have a multisystem neurologic disorder,<sup>9</sup> it is reasonable to also hypothesize a subclinical extravisual brain involvement in patients with *OPA1*-DOA.

The aim of the present study was to investigate the brain white matter of patients with *OPA1*-DOA compared with those with LHON and healthy controls, by using a voxelwise analysis of DTI, which can disclose abnormal water diffusivity in brain areas where atrophy and/or gliosis occur,<sup>10</sup> to look for subtle structural alterations.

## MATERIALS AND METHODS

### Subjects

Between October 2008 and May 2012, 19 adult patients with a definite diagnosis of *OPA1*-DOA and 17 adult patients with LHON were recruited for DTI evaluation. Inclusion criteria were 18 years of age and older, absence of white matter abnormalities as reported by previous conventional MR imaging, and availability of a genetic diagnosis. In addition, 19 control subjects with similar demographic characteristics were recruited within the same period. The characteristics of these cohorts are reported in and Online Tables 1 and 2. All subjects gave written informed consent, and the local institutional review board approved the study.

### MR Imaging Acquisition

Each subject underwent MR imaging examination by using a 1.5T Signa HDx scanner (GE Healthcare, Milwaukee, Wisconsin), with a protocol that included the following sequences: T2-weighted FLAIR (TR/TE/TI, 8000/85/2000 ms; axial FOV, 24 cm; 256 × 256 in-plane resolution; 3-mm sections); T2-weighted FSE (TR, 5.6–6.5 seconds; TE, 107 ms; coronal FOV, 24 cm; 256 × 256 in-plane resolution; 4-mm sections); T1-weighted volumetric imaging (fast-spoiled gradient recalled imaging; TR/TE, 12.3/5.2 ms; 1-mm isotropic resolution); DTI (TR/TE, 10,000/82 ms; 7 + 64 acquisitions with noncollinear field gradients; b-value = 0 or 900 s mm<sup>-2</sup>; axial oblique FOV, 32 cm; 128 × 128 in-plane resolution; 3-mm sections). Conventional images were evaluated to confirm the absence of white matter lesions. None of the subjects studied showed evidence of such abnormalities.

### DTI Data Processing

Following affine registration of all volumes to the first (by using eddy\_correct; fMRI of the Brain Software Library[FSL]; [\[www.fmrib.ox.ac.uk/fsl\]\(http://www.fmrib.ox.ac.uk/fsl\)\) to account for eddy current effects and subject motion, DTI data were processed to provide voxelwise estimates of tensor parameters, including mean diffusivity \(MD\) and fractional anisotropy \(FA\). FA and MD volumes from each subject were rigidly aligned to a standard template by using the fMRI of the Brain Linear Image Registration Tool \(FLIRT; <http://www.fmrib.ox.ac.uk>\) with 6 df. FA and MD volumes were jointly registered by nonlinear deformation \(Diffeomorphic Anatomical Registration Through Exponentiated Lie Algebra Toolbox, SPM8; <http://www.fil.ion.ucl.ac.uk/spm/software/spm8>\) to a study-specific template generated by using data from all study participants. Major white matter tracts were identified by using the tract-based spatial statistics \(TBSS\) procedure \(in FSL\), by using high-diffusion anisotropy as a marker of uniform fiber orientation, with an FA threshold of 0.2.](http://</a></p></div><div data-bbox=)

### DTI Statistical Analysis

The focus of the statistical analysis was to identify areas showing altered white matter compared with the control group and relate such alterations to relevant clinical and genetic factors. Nonparametric statistical inference was performed on the basis of a generalized linear model framework (by using Randomize; <http://fsl.fmrib.ox.ac.uk/fsl/fslwiki/randomize>, with cluster-free enhancement),<sup>11</sup> yielding voxelwise probability estimates, adjusted by controlling the family-wise error rate. After intermediate processing, described above, DTI data were analyzed in 2 stages. In the first stage, group differences between each patient group and controls were assessed (for voxels within the TBSS mask) by using a single-sided *t* test. We assumed that MD should increase and FA, decrease in patients compared with controls on the basis of previous observations of degenerative brain disease.<sup>12</sup> Voxels showing a difference at *P* < .05 after family-wise error correction were deemed significantly altered. To reduce the possible confounding effect of demographic factors, we embedded the *t* test in an ANCOVA-type analysis, first with age and sex as covariates, and repeated it with a history of idebenone therapy as a potential additional confounder. Because 3 patients with *OPA1*-DOA (patients 4, 6, and 7; Online Table 1) presented with an arguably distinct pathology, we reran the analysis, placing these participants in a separate group, to exclude the possibility that they alone were driving any possible group differences between *OPA1*-DOA and healthy control groups.

To summarize findings, we classified voxels within the TBSS white matter skeleton as belonging to the optic radiation (OR) or to other white matter bundles, by using standard FSL brain atlases,<sup>13–15</sup> and checked them by back-projecting the resulting labels onto the original individual FA images, to guard against possible tract misidentification.<sup>16</sup> The number of significantly abnormal OR voxels is also reported as a fraction of all abnormal voxels.

We assumed that given the relatively low sensitivity of (appropriately corrected) voxel-based statistical analysis, correlations between altered tissue microstructure and underlying causative variables might be apparent in the patient groups, even in regions not showing significant differences from healthy controls. Hence, in parallel, exploratory regression analysis was performed for FA and MD for all voxels within the previously identified major white matter tracts, against clinical and genetic factors with a known or

putative importance in determining the phenotype of the pathology under consideration. Results were not corrected for multiple comparisons beyond voxelwise family-wise error correction.

For both patient groups, subject age, estimated age at onset of symptoms, and disease duration were considered. In addition, a regression on control subject age was performed as a baseline check. Indicators of visual system involvement in disease progression, visual acuity, and retinal nerve fiber layer (RNFL) thickness assessed by optical coherence tomography<sup>17</sup>—specifically the average and temporal quadrant RNFL thickness—were used to perform a linear regression.

Categoric factors potentially modifying disease natural history were identified and analyzed by using a *t* test. These were the mitochondrial DNA haplogroup and a history of idebenone therapy.

*OPA1* mutations were grouped as either missense or haploinsufficiency on the basis of their pathogenic mechanism and under the hypothesis that the haploinsufficiency mutations would result in a less severe disease phenotype.<sup>9</sup> For patients with LHON only, the history of visual recovery was considered as an additional factor for a subgroup *t* test.

## RESULTS

Most patients with LHON had the 11778 ND4 mutation (13 of 17), whereas 17 different *OPA1* mutations were found among the patients with *OPA1*-DOA (On-line Table 1). Data regarding the mitochondrial DNA haplogroup, a potential modifying factor in either disorder, were also available for patients and showed the expected variation in a population of European descent, with preponderant occurrence of the most common haplogroup H (On-line Table 1). Three patients with *OPA1*-DOA had extravisual symptoms (patients 4, 6, and 7; On-line Table 1) and were classified as “plus.” Eleven patients with LHON and 9 patients with *OPA1*-DOA were administered idebenone (270–675 mg/day) (On-line Table 1). Data on visual acuity and RNFL thickness were available for almost all patients, though with variable timing with respect to the scan, and are presented in On-line Table 2.

In total, the white matter skeleton generated by TBSS covered 132,617 voxels, of which 12% were estimated as belonging to the OR; 1.9%, to the acoustic radiation; and the remainder, to other white matter bundles.

### Group Comparisons

Patients with *OPA1*-DOA and LHON showed significant increases in white matter MD and decreases in FA compared with controls (Table 1). For both patient groups, FA was the more severely affected in almost all areas. The number of voxels with a significant difference in terms of diffusivity parameters was considerably higher in patients with *OPA1*-DOA than in those with LHON. Furthermore, in the patients with LHON, half of these voxels were within the OR and the other half were within other white matter areas, in which the acoustic radiation was the most consistent, affected bilaterally (3.5% of all affected voxels, for FA), while the remainder included the superior corona radiata, superior longitudinal fasciculus, and medial corpus callosum only in the right side (Figs 1 and 2A, -C). The results were different in patients with *OPA1*-DOA, given that only one-fifth of the voxels affected belonged

**Table 1: Significant results of a *t* test for comparison of DTI parameters between patients and controls**

Quantity	Contrast	Whole White Matter Skeleton <sup>a</sup>		
		Voxels	%	Threshold <i>t</i>
FA	Controls > LHON	7310	5.5	1.54
	Controls > <i>OPA1</i> -DOA <sup>b</sup>	40,197	30.3	1.02
	Controls > pure <i>OPA1</i> -DOA <sup>c</sup>	19,006	14.3	1.18
MD	LHON > controls	652	0.5	0.95
	<i>OPA1</i> -DOA > controls <sup>b</sup>	38,789	29.2	2.33
	Pure <i>OPA1</i> -DOA > controls <sup>c</sup>	19,170	14.5	1.13

<sup>a</sup> Results are expressed as the number of voxels within the TBSS skeleton showing significant differences, along with the percentage so affected.

<sup>b</sup> All patients included.

<sup>c</sup> Three cases with *OPA1* plus are excluded.

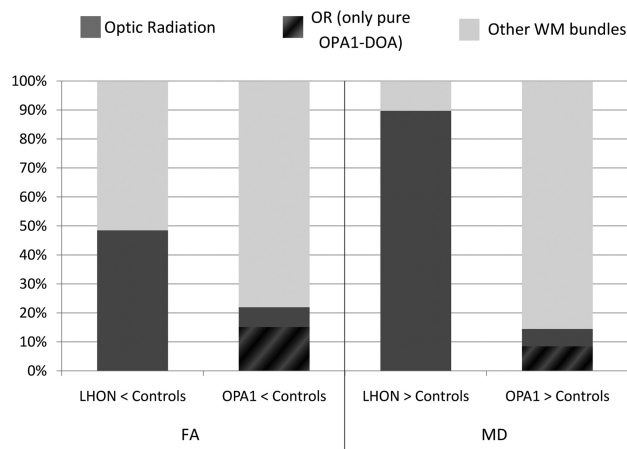


**FIG 1.** The number of significantly abnormal OR voxels as a proportion of all abnormal voxels in patients with LHON and *OPA1*-dominant optic atrophy.

to the OR, while most were distributed evenly throughout the whole white matter, including several areas not involved in patients with LHON and involving almost all bundles within the supratentorial and infratentorial compartments (Figs 1 and 2B, -D). On-line Figs 1–6 show the complete set of results for both groups.

For the comparison of patients with LHON and controls, the inclusion of treatment with idebenone as a covariate increased the number of affected voxels (by 45% for FA and 175% for MD, dispersed both within and beyond the OR), while for those with *OPA1*-DOA compared with controls, there was essentially no change (–1.7% and 0.9%, respectively).

If we excluded the patients with *OPA1* “plus” (with nonvisual symptoms) from the analysis, the decrease in FA and increase in MD remained in about half the voxels that were altered for the whole group of patients with *OPA1*-DOA compared with controls (Table 1). The proportion of altered voxels outside the OR remained similar (Fig 1). FA values were lower for “plus” compared with nonsyndromic patients at the level of the right internal and external capsules, left OR, and splenium of corpus callosum bilaterally.

### Regression Analysis

Exploratory regression analyses are summarized in Table 2 and revealed a highly significant reduction in FA with age in patients with *OPA1*-DOA in almost all of the areas considered. The regression of FA on subject age for the control group was negative,



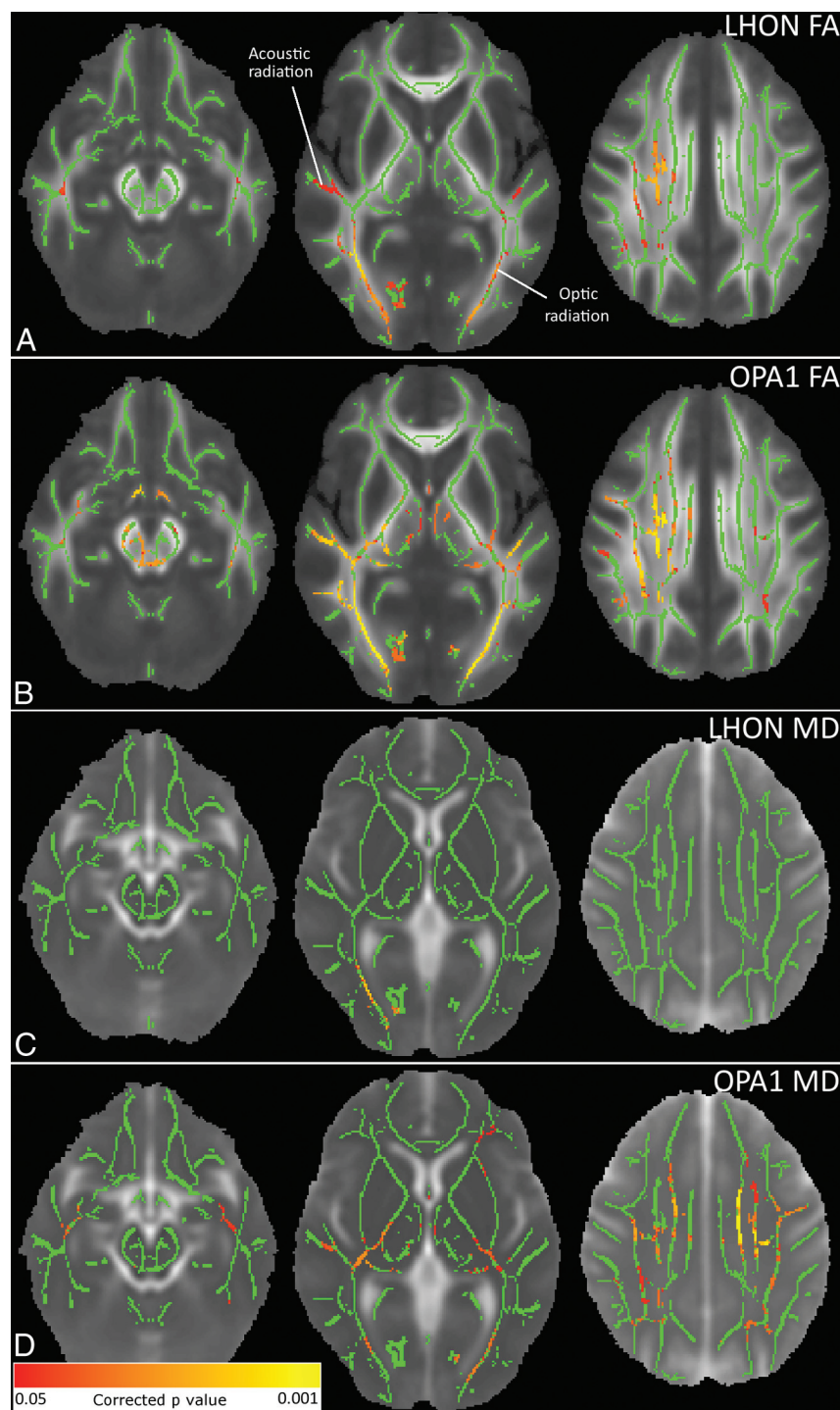


**FIG 2.** Representative axial sections are shown on the white matter tract skeleton (in green) projected onto the mean FA and MD maps. Voxels showing significant differences between patients and controls (corrected  $P < .05$ ) are shown in a red-yellow scale. **A**, LHON FA < control FA: bilateral optic and acoustic radiation and right superior corona radiata, superior longitudinal fasciculus, and middle corpus callosum were significant. **B**, OPA1-DOA FA < control FA: widespread reduction of FA involving almost all white matter bundles was present. **C** and **D**, Patient MD > control MD: increased MD was found in the same areas where FA was reduced, though to a lesser extent, in both groups of patients. Complete results in both groups of patients are shown in On-line Figs 1–6.

strengthening the likelihood that the positive finding for patients with OPA1-DOA was group-specific. MD was higher in patients with OPA1-DOA with a missense mutation compared with those with haploinsufficiency mutations (mean WM skele-

ton value,  $0.815 \pm 0.229$  versus  $0.741 \pm 0.170 \times 10^{-3} \text{mm}^2 \text{s}^{-1}$ ), and again this finding was true of the OR and almost all other WM areas. In addition, FA values directly correlated with average RNFL thickness in several areas, mostly within the OR, optic tract, internal and external capsules, and corona radiata bilaterally. A trend toward higher MD values ( $P = .05$ , corrected) was evident in patients with OPA1-DOA with worse visual acuity, at the level of the anterior cingulum, genu of corpus callosum, and prefrontal WM of the left side. Other trends ( $.05 < P < .07$ , corrected) were disclosed in patients with OPA1-DOA. Specifically, disease duration was diffusely and inversely correlated with FA values (prevalent in the right hemisphere); finally, FA values in the genu of corpus callosum were higher in patients taking idebenone compared with untreated patients (mean corpus callosum WM skeleton value,  $0.745 \pm 0.087$  versus  $0.618 \pm 0.136$ ).

Considering patients with LHON, the only significant regression analysis was for idebenone therapy, showing that patients taking idebenone had lower MD values within the anterior cingulum ( $0.750 \pm 0.035$  versus  $0.773 \pm 0.039$ ), genu of corpus callosum ( $0.784 \pm 0.071$  versus  $0.814 \pm 0.058$ ), olfactory tracts bilaterally ( $0.750 \pm 0.120$  versus  $0.769 \pm 0.095$ ), and in the left prefrontal WM ( $0.728 \pm 0.053$  versus  $0.740 \pm 0.045$ ) compared with untreated patients. No other regression analysis yielded positive results.

## DISCUSSION

In this study, we evaluated the integrity of brain WM in patients with mitochondrial optic neuropathies, by using a voxelwise analysis of DTI, demonstrating that in both LHON and OPA1-DOA, there are pathologic changes, but with a different distribution. Patients with LHON showed abnormal diffusion mainly in the bilateral OR, with some involvement of the acoustic radiation and a few other areas. In contrast, patients with OPA1-DOA showed changes not only in the OR but also throughout

much of the white matter, indicating a widespread pathology affecting the central nervous system.

The involvement of the OR in patients with LHON confirms and extends the results of recent imaging studies,<sup>5–7</sup> suggesting

**Table 2: Significant results of analyses of DTI parameters for patient groups**

	Quantity	Explanatory Variable	Test	Threshold <i>P</i> Value	% Suprathreshold Voxels <sup>a</sup>	Threshold <i>r</i> <sup>b</sup>
OPA1-DOA	FA	Age	Regression	.05	14.5%	−0.299
		Mean RNFL	Regression	.05	8.0%	+0.318
		Disease duration	Regression	.07 <sup>c</sup>	7.1%	+0.224
		Idebenone	<i>t</i> test	.07 <sup>c</sup>	0.6%	NA
	MD	Mutation	<i>t</i> test	.05	60.8%	NA
LHON	MD	Visual acuity	Regression	.07 <sup>c</sup>	31.0%	+0.224
		Idebenone	<i>t</i> test	.05	4.2%	NA

<sup>a</sup> Results are expressed as the percentage of voxels within the TBSS skeleton showing *P* value indicated.

<sup>b</sup> *R* indicates the Pearson product moment correlation coefficient.

<sup>c</sup> Trend finding.

the probable trans-synaptic nature of this impairment. This interpretation was supported by a postmortem investigation in 1 case of LHON, detecting atrophy (40%–45% decrease of neuron soma size) and, to a lesser extent, degeneration (approximately a 28% decrease of neuron attenuation) in the lateral geniculate nucleus, in contrast to the extremely severe axonal loss (99%) in the optic nerve.<sup>6</sup> In one of these imaging studies, the reduced attenuation of the OR detected by voxel-based morphometry analysis correlated with the average and temporal RNFL thickness.<sup>5</sup> This correlation was not apparent in the previous DTI study on the same patients<sup>7</sup> or in our study, though missing ophthalmologic data for a few patients and the variable timing with respect to the scan could have affected our regression analysis.

Our results also demonstrate the bilateral involvement of the acoustic radiation in patients with LHON, a finding not apparent in previous studies in which whole-brain analysis was performed. The presence of auditory dysfunction in LHON had been studied in the past, with conflicting results. An early study found auditory brain stem–evoked potential abnormalities in 7 of 11 patients,<sup>18</sup> and subsequently 2 cases of LHON with auditory neuropathy were reported.<sup>19</sup> A further study on a sample of 10 patients found no evidence of auditory neural abnormalities,<sup>20</sup> while a more recent study on 48 subjects carrying a LHON mutation disclosed that >25% of both symptomatic and asymptomatic participants showed electrophysiologic evidence of auditory neuropathy with either absent or severely delayed auditory brain stem potentials.<sup>21</sup> Our current results of white matter changes in the auditory radiation may represent the auditory counterpart of the trans-synaptic degeneration attributable to the OR.

Furthermore, we have found some other brain diffusion changes in LHON at the level of the right superior corona radiata, superior longitudinal fasciculus, and medial corpus callosum. These results are more difficult to interpret but may indicate a microscopic and diffuse, though variable, white matter pathology associated with the primary mitochondrial impairment. This was previously suggested by older studies using phosphorus MR spectroscopy to show bioenergetic dysfunction in the occipital lobes<sup>22</sup> and mild abnormalities of the whole normal-appearing white matter using histogram analysis of magnetization transfer imaging and DWI.<sup>23</sup> These findings may also relate to the occasional co-occurrence of a multiple sclerosis–like illness in patients with LHON,<sup>24</sup> in which an autoimmune process could be triggered by the release of immunogenic material due to myelin damage caused by mitochondrial dysfunction in the presence of a specific predisposition.<sup>25</sup>

Most interesting, in patients with LHON treated with ide-

benone, the MD values within the anterior cingulum, genu of corpus callosum, olfactory tracts bilaterally, and left prefrontal WM were lower compared with untreated patients. Conversely, patient-control differences were more readily apparent when idebenone treatment was included as a confounding factor. Although this result should be considered with caution, it is compatible with previous clinical evidence of the partial efficacy of idebenone treatment in LHON.<sup>26,27</sup>

However, the most interesting findings of the current study concern our results in OPA1-DOA, to our knowledge the first for this patient group based on DTI. We found widespread WM diffusivity changes without a clear prevalence in a specific pathway. This finding implies that besides trans-synaptic degeneration, there is also a primary WM pathology involving multiple brain systems, a finding in close agreement with the mounting clinical evidence that subjects carrying OPA1 mutations may have a multisystem neurologic disease (DOA “plus”), including sensorineural deafness, ataxia, sensory-motor polyneuropathy, chronic progressive external ophthalmoplegia, and mitochondrial myopathy,<sup>9,28,29</sup> in addition to optic atrophy. Other reported clinical presentations may include spastic paraparesis mimicking hereditary spastic paraplegia,<sup>9</sup> multiple sclerosis–like illness,<sup>9,30</sup> cervical dystonia,<sup>31</sup> and even a multisystemic disorder in the absence of optic atrophy.<sup>32</sup> Furthermore, patients with “pure” optic atrophy may have evidence of subclinical corticospinal tract involvement as shown by electrophysiologic evaluation.<sup>33</sup> All these observations fit well with our finding of subclinical impairment of several white matter pathways, which correlates with optic atrophy, as quantified by the average RNFL thickness. These observations are consistent with white matter sensitivity to mitochondrial dysfunction.<sup>1,25</sup> In particular, complex I deficiency, as obviously occurring in LHON and also demonstrated in OPA1-DOA with haploinsufficiency,<sup>34</sup> is frequently associated with leukoencephalopathy or other white matter pathology.<sup>35</sup> Most interesting, recent studies propose that myelin itself has an autonomous respiratory activity, thus linking white matter integrity to defective oxidative phosphorylation.<sup>36</sup>

An interesting and strong correlation was found between diffusivity parameters and age for patients with OPA1-DOA, but not for those with LHON or healthy controls, suggesting a disease-specific association. The absence of a correlation with “apparent” disease duration ( $.05 < P < .07$  in the same areas) and the difficulty of accurately defining the onset of this insidious disease in clinical practice suggest that OPA1-DOA may be a congenital disease. Indeed, it has been shown that patients have a significantly smaller optic nerve head compared with controls, leading to the

hypothesis of a developmental disorder.<sup>37</sup> In addition, the role of the *OPA1* protein in controlling apoptosis is well-documented,<sup>38,39</sup> and it may be postulated that *OPA1* mutations alter the pattern of developmental apoptosis during embryonic stages leading to a congenital “weakness” of the optic nerve and other brain structures.

Almost all WM areas in patients with *OPA1*-DOA had higher MD values in the presence of a missense mutation compared with those predicted to lead to haploinsufficiency. This finding is not surprising because the occurrence of clinical multisystem neurologic disease, though associated with all mutational subtypes, has been reported to be increased 3-fold with missense mutations.<sup>9</sup> The 3 patients with DOA “plus” tended to have greater pathologic changes compared with nonsyndromic patients, both within and beyond the OR. The findings regarding the effect of idebenone treatment are inconclusive but give limited support to previous preliminary clinical results showing a slight improvement of visual function in patients with DOA after idebenone therapy.<sup>40</sup>

## CONCLUSIONS

Voxelwise analysis of DTI was used to evaluate brain WM integrity in patients with LHON and, for the first time, in patients with *OPA1*-DOA, with clear-cut differences between the 2 disorders. Patients with LHON presented with a preferential involvement of the optic and acoustic radiations, possibly due to trans-synaptic degeneration. Patients with *OPA1*-DOA presented with a widespread WM involvement, supporting the view of *OPA1*-associated disorders as a multisystemic disease, not merely limited to the optic nerve. The strong and specific correlation between diffusivity abnormalities and the age of these patients also supports the hypothesis of a congenital and developmental disorder, an issue that will require further investigation. Finally, our study shows that DTI can evaluate white matter integrity in mitochondrial optic neuropathies and may yield useful surrogate biomarkers of disease severity and progression, to evaluate therapeutic efficacy in these mitochondrial optic neuropathies.

Disclosures: David N. Manners—OTHER RELATIONSHIPS: The study was financially supported in part by Telethon-Italy grants GGP06233 and GPPI0005 and by E-RARE project ERMION (European Research project on Mendelian Inherited Optic Neuropathies); OIGMI006. The funding organizations played no part in the design or conduct of the study; collection, management, analysis, or interpretation of the data; or in the preparation, review, or approval of the manuscript. Valerio Carelli—RELATED: Grant: Telethon Italy grants GGP06233 and GPPI0005,\* and E-RARE project ERMION: OIGMI006,\* Comments: grants to Valerio Carelli for research on inherited optic neuropathies; UNRELATED: Grants/Grants Pending: Program ER-MITO from the Italian region Emilia Romagna, Comments: This is a Program Project for epidemiology on mitochondrial diseases in the Italian region Emilia Romagna; OTHER RELATIONSHIPS: currently involved in clinical trials with EPI-743 ( $\alpha$ -tocotrienol quinone) in Leber hereditary optic neuropathy (Edison Pharmaceuticals, Mountain View, California) and with l-acetyl carnitine in Leber hereditary optic neuropathy (Sigma-Tau, Italy). \*Money paid to the institution.

## REFERENCES

1. Carelli V, Ross-Cisneros FN, Sadun AA. Mitochondrial dysfunction as a cause of optic neuropathies. *Prog Retin Eye Res* 2004;23:53–89
2. Yu-Wai-Man P, Griffiths PG, Chinnery PF. Mitochondrial optic neuropathies: disease mechanisms and therapeutic strategies. *Prog Retin Eye Res* 2011;30:81–114
3. Sadun AA, Win PH, Ross-Cisneros FN, et al. Leber's hereditary optic neuropathy differentially affects smaller axons in the optic nerve. *Trans Am Ophthalmol Soc* 2000;98:223–32
4. Pan BX, Ross-Cisneros FN, Carelli V, et al. Mathematically modeling the involvement of axons in Leber's hereditary optic neuropathy. *Invest Ophthalmol Vis Sci* 2012;53:7608–17
5. Barcella V, Rocca MA, Bianchi-Marzoli S, et al. Evidence for retinohypothalamic tissue loss in Leber's hereditary optic neuropathy. *Hum Brain Mapp* 2010;31:1900–06
6. Rizzo G, Tozer KR, Tonon C, et al. Secondary post-geniculate involvement in Leber's hereditary optic neuropathy. *PLoS One* 2012;7:e50230
7. Milesi J, Rocca MA, Bianchi-Marzoli S, et al. Patterns of white matter diffusivity abnormalities in Leber's hereditary optic neuropathy: a tract-based spatial statistics study. *J Neurol* 2012;259:1801–07
8. Bette S, Schlasz H, Wissinger B, et al. *OPA1*, associated with autosomal dominant optic atrophy, is widely expressed in the human brain. *Acta Neuropathol* 2005;109:393–99
9. Yu-Wai-Man P, Griffiths PG, Gorman GS, et al. Multi-system neurological disease is common in patients with *OPA1* mutations. *Brain* 2010;133:771–86
10. Pierpaoli C, Jezzard P, Basser PJ, et al. Diffusion tensor MR imaging of the human brain. *Radiology* 1996;201:637–48
11. Winkler A, Ridgway G, Webster M, et al. Permutation inference for the general linear model. *Neuroimage* 2014;92:381–97
12. Nucifora PG, Verma R, Lee SK, et al. Diffusion-tensor MR imaging and tractography: exploring brain microstructure and connectivity. *Radiology* 2007;245:367–84
13. Mori S, Wakana S, van Zijl PC, et al. *MRI Atlas of Human White Matter*. Amsterdam: Elsevier; 2005
14. Hua K, Zhang J, Wakana S, et al. Tract probability maps in stereotaxic spaces: analyses of white matter anatomy and tract-specific quantification. *Neuroimage* 2008;39:336–47
15. Eickhoff SB, Stephan KE, Mohlberg H, et al. A new SPM toolbox for combining probabilistic cytoarchitectonic maps and functional imaging data. *Neuroimage* 2005;25:1325–35
16. Bach M, Laun FB, Leemans A, et al. Methodological considerations on tract-based spatial statistics (TBSS). *Neuroimage* 2014;100:358–69
17. Barboni P, Savini G, Parisi V, et al. Retinal nerve fiber layer thickness in dominant optic atrophy measurements by optical coherence tomography and correlation with age. *Ophthalmology* 2011;118:2076–80
18. Mondelli M, Rossi A, Scarpini C, et al. BAEP changes in Leber's hereditary optic neuropathy—further confirmation of multisystem involvement. *Acta Neurol Scand* 1990;81:349–53
19. Ceranić B, Luxon LM. Progressive auditory neuropathy in patients with Leber's hereditary optic neuropathy. *J Neurol Neurosurg Psychiatry* 2004;75:626–30
20. Yu-Wai-Man P, Elliot C, Griffiths PG, et al. Investigation of auditory dysfunction in Leber hereditary optic neuropathy. *Acta Ophthalmol* 2008;86:630–33
21. Rance G, Kearns LS, Tan J, et al. Auditory function in individuals within Leber's hereditary optic neuropathy pedigrees. *J Neurol* 2012;259:542–50
22. Cortelli P, Montagna P, Avoni P, et al. Leber's hereditary optic neuropathy: genetic, biochemical, and phosphorus magnetic resonance spectroscopy study in an Italian family. *Neurology* 1991;41:1211–15
23. Inglese M, Rovaris M, Bianchi S, et al. Magnetic resonance imaging, magnetisation transfer imaging, and diffusion weighted imaging correlates of optic nerve, brain, and cervical cord damage in Leber's hereditary optic neuropathy. *J Neurol Neurosurg Psychiatry* 2001;70:444–49
24. Harding AE, Sweeney MG, Miller DH, et al. Occurrence of a multiple sclerosis-like illness in women who have a Leber's hereditary optic neuropathy mitochondrial DNA mutation. *Brain* 1992;115:979–89
25. Carelli V, Bellan M. Myelin, mitochondria, and autoimmunity: what's the connection? *Neurology* 2008;70:1075–76
26. Klopstock T, Yu-Wai-Man P, Dimitriadis K, et al. A randomized placebo-controlled trial of idebenone in Leber's hereditary optic neuropathy. *Brain* 2011;134:2677–86



27. Carelli V, La Morgia C, Valentino ML, et al. **Idebenone treatment in Leber's hereditary optic neuropathy.** *Brain* 2011;134:e188
28. Hudson G, Amati-Bonneau P, Blakely EL, et al. **Mutation of OPA1 causes dominant optic atrophy with external ophthalmoplegia, ataxia, deafness and multiple mitochondrial DNA deletions: a novel disorder of mtDNA maintenance.** *Brain* 2008;131:329–37
29. Amati-Bonneau P, Valentino ML, Reynier P, et al. **OPA1 mutations induce mitochondrial DNA instability and optic atrophy 'plus' phenotypes.** *Brain* 2008;131:338–51
30. Verny C, Loiseau D, Scherer C, et al. **Multiple sclerosis-like disorder in OPA1-related autosomal dominant optic atrophy.** *Neurology* 2008;70:1152–53
31. Liskova P, Ulmanova O, Tesina P, et al. **Novel OPA1 missense mutation in a family with optic atrophy and severe widespread neurological disorder.** *Acta Ophthalmol* 2013;91:e225–31
32. Milone M, Younge BR, Wang J, et al. **Mitochondrial disorder with OPA1 mutation lacking optic atrophy.** *Mitochondrion* 2009;9: 279–81
33. Baker MR, Fisher KM, Whittaker RG, et al. **Subclinical multisystem neurologic disease in "pure" OPA1 autosomal dominant optic atrophy.** *Neurology* 2011;77:1309–12
34. Zanna C, Ghelli A, Porcelli AM, et al. **OPA1 mutations associated with dominant optic atrophy impair oxidative phosphorylation and mitochondrial fusion.** *Brain* 2008;131:352–67
35. Koene S, Rodenburg RJ, van der Knaap MS, et al. **Natural disease course and genotype-phenotype correlations in complex I deficiency caused by nuclear gene defects: what we learned from 130 cases.** *J Inherit Metab Dis* 2012;35:737–47
36. Morelli A, Ravera S, Panfoli I. **Hypothesis of an energetic function for myelin.** *Cell Biochem Biophys* 2011;61:179–87
37. Barboni P, Carbonelli M, Savini G, et al. **OPA1 mutations associated with dominant optic atrophy influence optic nerve head size.** *Ophthalmology* 2010;117:1547–53
38. Frezza C, Cipolat S, Martins de Brito O, et al. **OPA1 controls apoptotic cristae remodeling independently from mitochondrial fusion.** *Cell* 2006;126:177–89
39. Cipolat S, Rudka T, Hartmann D, et al. **Mitochondrial rhomboid PARL regulates cytochrome c release during apoptosis via OPA1-dependent cristae remodeling.** *Cell* 2006;126:163–75
40. Barboni P, Valentino ML, La Morgia C, et al. **Idebenone treatment in patients with OPA1-mutant dominant optic atrophy.** *Brain* 2013; 136:e231